IOWA STATE UNIVERSITY
Digital Repository

Graduate Theses and Dissertations

Iowa State University Capstones, Theses and Dissertations

2017

Analysis of four-point alternating current potential drop measurements on an anisotropic conductive half-space

Tyler Douglas Antony
Iowa State University

Follow this and additional works at: https://lib.dr.iastate.edu/etd

 Part of the Electrical and Electronics Commons

Recommended Citation
Antony, Tyler Douglas, "Analysis of four-point alternating current potential drop measurements on an anisotropic conductive half-space" (2017). *Graduate Theses and Dissertations*. 16071.
https://lib.dr.iastate.edu/etd/16071

This Thesis is brought to you for free and open access by the Iowa State University Capstones, Theses and Dissertations at Iowa State University Digital Repository. It has been accepted for inclusion in Graduate Theses and Dissertations by an authorized administrator of Iowa State University Digital Repository. For more information, please contact digirep@iastate.edu.

Analysis of four-point alternating current potential drop measurements on an anisotropic conductive half space

by

Tyler D. Antony

A thesis submitted to the graduate faculty

inf partial fulfillment of the requirements for the degree of

MASTER OF SCIENCE

Major: Electrical Engineering

Program of Study Committee:
Nicola Bowler, Major Professor
Brian Hornbuckle
Jiming Song

The student author, whose presentation of the scholarship herein was approved by the program of study committee, is solely responsible for the content of this thesis. The Graduate College will ensure this thesis is globally accessible and will not permit alterations after a degree is conferred.

Iowa State University

Ames, Iowa

2017

Copyright © Tyler D. Antony, 2017. All rights reserved.

DEDICATION

To my mother and father.

TABLE OF CONTENTS

LIST OF TABLES

LIST OF FIGURES

ACKNOWLEDGEMENTS

Many people helped with my studies and the development of this thesis. I would like to thank Dr. Nicola Bowler for her valuable advice and guidance in the completion of this project. I would also like to thank the committee members, Dr. Brian Hornbuckle and Dr. Jiming Song, for teaching classes and for serving on my graduate committee. Amin Gorji also assisted with the thesis.

ABSTRACT

In this thesis, an analysis is carried out concerning the behavior of the electric field when a line current is extracted/injected perpendicularly into a uniaxially anisotropic half-space. Such a solution enables characterization of uniaxially anisotropic materials using alternating current methods. This problem has previously been solved for the case of an isotropic half space. This paper follows a parallel development to that presented by Bowler [J. Appl. Phys., 96, 4607-4613, 2004] in which a transverse magnetic potential formulation was employed to derive an analytic solution for the electric field and alternating current potential drop measured by a four-point probe in contact with an isotropic half-space conductor. Here, the case when conductivity is given by a diagonal matrix quantity is treated. This is done by first solving for the electric field in the case of a single wire, and then using superposition to obtain the electric field on the conductor surface with two wires representing the current injection/extraction seen in a four-point probe. Finally, an analytical expression for the potential drop measured between the pick-up pins of the probe is given.

CHAPTER 1. OVERVIEW

1.1 Introduction

In this thesis, the analytical tractability of solving for the potential drop of a four-point probe injecting and extracting current from an anisotropic conductive half-space is hypothesized. A solution to the problem is then derived.

Prajapati et al. (2) used alternating current potential drop (ACPD) to examine creep damage in materials. They found that creep damage could be characterized by anisotropic conductivity in materials. Tian et al. (3) sought to emulate material degradation in nuclear power plants by subjecting Fe-Cu alloy to thermal aging and cold work. The resulting material properties were then measured with pulsed eddy currents, with anisotropy being found to monotonically increase with the amount of cold work. Todorov (4) determined the electromagnetic properties of different types of heat exchanger tubes, including electrical conductivity. Anisotropy was found between the two different geometrical directions.

1.2 Maxwell's Equations

All classical electrodynamic problems can be solved by utilizing Maxwell's equations, which in time-harmonic form in a charge-free region are given by:

$$\nabla \times \vec{E} = i\omega\vec{B} \tag{1.1}$$

$$\nabla \times \vec{H} = \nabla \times \frac{\vec{B}}{\mu} = \vec{J} \tag{1.2}$$

$$\nabla \cdot \vec{E} = 0 \tag{1.3}$$

$$\nabla \cdot \vec{B} = 0 \tag{1.4}$$

where $\vec{E}$ is the electric field, $\vec{B}$ is the magnetic flux density, $\vec{H}$ is the magnetic field intensity, $\vec{J}$ is the current density, and μ is the permeability, here assumed to be isotropic. A time-dependence of $e^{-i\omega t}$ is assumed above. Maxwell's equations are often manipulated to obtain a single differential equation for $\vec{E}$. First, one takes the curl of (1.1), then substitutes for $\nabla \times \vec{B}$ from (1.2):

$$\nabla \times \nabla \times \vec{E} = i\omega \nabla \times \vec{B} = i\omega\mu\vec{J}. \tag{1.5}$$

In an anisotropic conductor, we have the constitutive relation:

$$\vec{J} = \bar{\bar{\sigma}} \cdot \vec{E} \tag{1.6}$$

where $\bar{\bar{\sigma}}$ is the tensor conductivity of the metal, given by the following in the case of uniaxial anisotropy:

$$\bar{\bar{\sigma}} = \begin{pmatrix} \sigma_{tt} & 0 & 0 \\ 0 & \sigma_{tt} & 0 \\ 0 & 0 & \sigma_{zz} \end{pmatrix}. \tag{1.7}$$

Using this result in (1.5), we obtain a single equation for $\vec{E}$ within a conductor:

$$\nabla \times \nabla \times \vec{E} - i\omega\mu\bar{\bar{\sigma}} \cdot \vec{E} = \nabla \times \nabla \times \vec{E} - \bar{\bar{k}}^2 \cdot \vec{E} = 0, \tag{1.8}$$

where $\bar{\bar{k}}^2 = i\omega\mu\bar{\bar{\sigma}}$. It will be useful to express $\bar{\bar{k}}^2$ in the form:

$$\bar{\bar{k}}^2 = \begin{pmatrix} k_{tt}^2 & 0 & 0 \\ 0 & k_{tt}^2 & 0 \\ 0 & 0 & k_{zz}^2 \end{pmatrix}. \tag{1.9}$$

Where $k_{tt}^2 = i\omega\mu\sigma_{tt}$ and $k_{zz}^2 = i\omega\mu\sigma_{zz}$. Noting the following vector identity:

$$\nabla \times \nabla \times \vec{F} = \nabla(\nabla \cdot \vec{F}) - \nabla^2\vec{F} \tag{1.10}$$

and then using (1.3) with (1.10) on (1.8) then gives:

$$\nabla^2 \vec{E} + \bar{\bar{k}}^2 \cdot \vec{E} = 0. \tag{1.11}$$

1.3 General Boundary Conditions

The general charge-free interface conditions on time-harmonic electromagnetic fields between two regions 1 and 2, Figure 1.1 are given by:

$$\hat{n} \times (\vec{E_2} - \vec{E_1}) = 0 \tag{1.12}$$

$$\hat{n} \times (\vec{H_2} - \vec{H_1}) = \vec{J_s} \tag{1.13}$$

$$\hat{n} \cdot (\vec{D_2} - \vec{D_1}) = 0 \tag{1.14}$$

$$\hat{n} \cdot (\vec{B_2} - \vec{B_1}) = 0 \tag{1.15}$$

where $\hat{n}$ is the unit vector normal to the interface between the two materials and $\vec{J_s}$ is the surface current density on the interface. In the problem to be solved, the governing equation for the electric field (1.11) can be used to find a governing equation for a potential in a source-free anisotropic medium. Then, the boundary condition for the current given in (1.12) is applied in conjunction with (1.6).

1.4 Overview

The geometry of the system to be solved consists of two primary components. The first component is a conductive anisotropic half-space characterized by a uniaxial tensor conductivity $\bar{\bar{\sigma}}$, given in (1.9). The second component is a wire of radius a injecting a time-harmonic current $Ie^{-i\omega t}$ perpendicularly into the conducting space. This configuration is illustrated in Figure (1.1). The electric field governing equation is re-framed in terms of a potential using the same potential formulation as two papers. For the isotropic case, the potential given by Bowler 2004

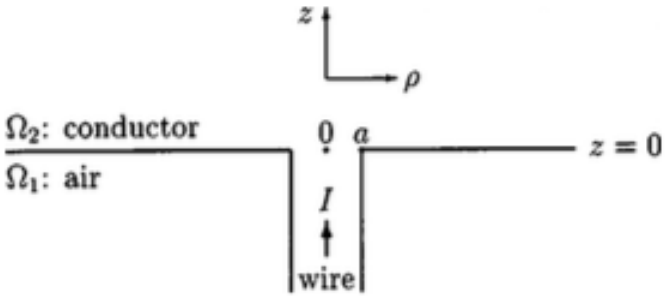

Figure 1.1: Cross section of wire of radius a carrying current I into a conductive half-space, taken from Bowler 2004 (8).

(8) is used. For the anisotropic conductor, a modified version of the potential given in the book by Felsen and Marcuvitz (14) is used.

Focusing on the conducting region, a governing equation for the potential that will be defined later is transformed using the Hankel transform. The boundary condition (1.12) is then used to find a solution for the potential. The electric field components are then found in terms of the potential, for which a solution is available in closed form.

The potential drop in the practical case of a four-point probe is then found by superposition of one configuration which describes injecting current and one configuration which describes extracting current. The line integral of the superposed field between two other points p and q which denote the positions of the pickup pins then gives the potential drop that can be measured, as shown in Figure 1.2.

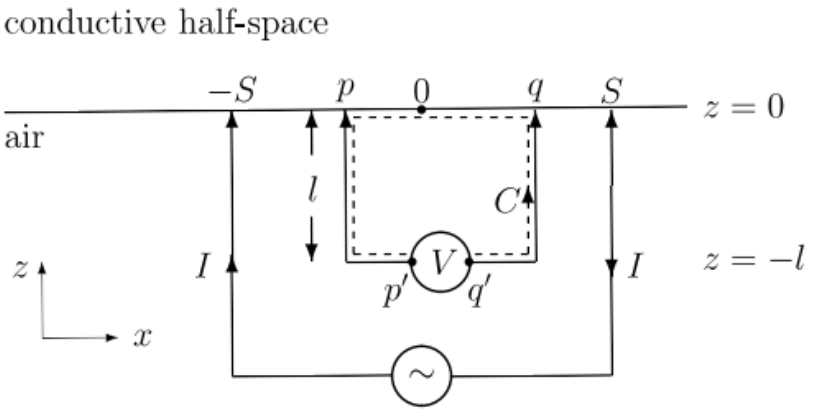

Figure 1.2: Four-point probe configuration with current injected/extracted at $(\pm S, 0, 0)$ and potential drop measured by pins at $x = p$ and $x = q$, taken from (19).

CHAPTER 2. REVIEW OF LITERATURE

2.1 Introduction

Potential drop methods are a set of non-destructive evaluation techniques that detect defects and characterize materials by using an apparatus, consisting of a number of electrodes, that passes current through the material and the electrodes and then measures the resulting potential drop. In full generality, a three-dimensional potential field is created by the current source and conductor, whose variations are then measured. If we consider a crack of depth d, and make the simplifying assumption that the voltage V is directly proportional to the distance between probes, then assuming that the probes are a distance l apart on the surface, we have the relationship (1):

$$\frac{V_0}{l} = \frac{V_1}{l + 2d}$$

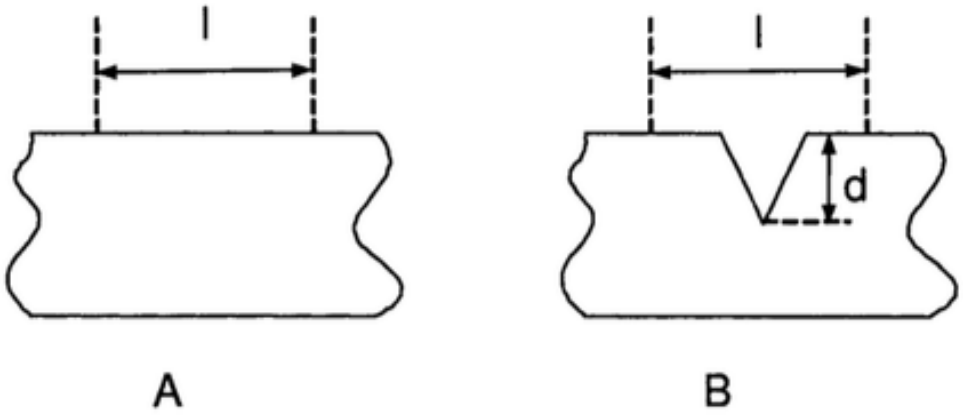

Figure 2.1: Simple heuristic for how a potential drop methods are utilized in non-destructive evaluation. Taken from Huang 2004 (1).

This model, while overly simplified, serves as a reasonable qualitative heuristic for how the measurement determines the quality of defects on conductive surfaces, and is most accurate for cracks that are larger than the pin separation and for frequencies sufficiently high that the current flows in a thin skin near to the conductor surface and crack faces.

2.1.1 Motivation/Examples

Several different examples of potential drop methods and their measurements will be examined in detail in what follows. Potential drop methods have been used to detect cracks in materials via the mechanism mentioned in the previous subsection (6) (7). Potential drop has also been used to characterize the properties of materials, including brass, aluminum, spring steel, and carbon steel with precision better than that of eddy current techniques (10). As shown below, transient potential drop methods could allow for the examination of layered inhomogeneous media (11).

Related to the focus of this thesis on anisotropic materials, a model of uniaxial stress on materials, that leads to anisotropy in electrical and magnetic parameters, is also summarized.

2.1.2 Four Point Probes Versus Two Point Probes

Use of four point probes is more accurate than two point probes. The underlying reason for this is that there are resistance terms that are extremely difficult to estimate accurately that arise when one uses the same electrodes to inject/extract current and measure potential drop.

2.2 Direct Current (DC) Potential Drop

2.2.1 Description and Comparison to Other Methods

In direct current potential drop (DCPD), the current running through the apparatus and sample is direct current. Typically, two pairs of probes straddle the cracks. One pair sends a direct current through the conductor, while another pair of electrodes straddles the crack and measures the potential difference across it (5). The DCPD method is good for finding hidden defects and for full automation of the measurement process (5). One common source of error in DCPD methods is the thermoelectric effect, which is a potential difference caused by

varying temperature. (6). The need for good electrical contacts with the sample also precludes the possibility of scanning for defects, since dragging the contact across the surface would be damaging to the probe and/or test-piece (5). Measurements are often conducted by calibrating the main measurement probe to a reference probe which is placed in a defect-free region and comparing the measured signals with each other (5) (6).

2.2.2 Measurement Examples

Yee and Lambert (6) conducted measurements on steel-welded T-joints. One purpose of their work was to obtain a picture of early fatigue crack development in steel structures which researchers could then use to improve their subsequent modelling of defect formation. A bending load was placed upon the joints by servohydraulic test rigs. The loading function was sinusoidal, meaning that stress was taken on and off periodically, at a frequency of 1 to 3 Hz. A reversing DCPD system (one which periodically reversed the polarity of the DC current) was used in order to counteract the error caused by thermoelectric voltage. A voltage was taken that was compared to a reference voltage measured in a defect-free area. The result was a prediction of crack depth generated by the DCPD system, which was then compared to ink stains or beachmarks observed after failure. The predictions obtained from the DCPD measurements were in agreement with the ink stain/beachmark measurements of the crack depth (Figure 2.2).

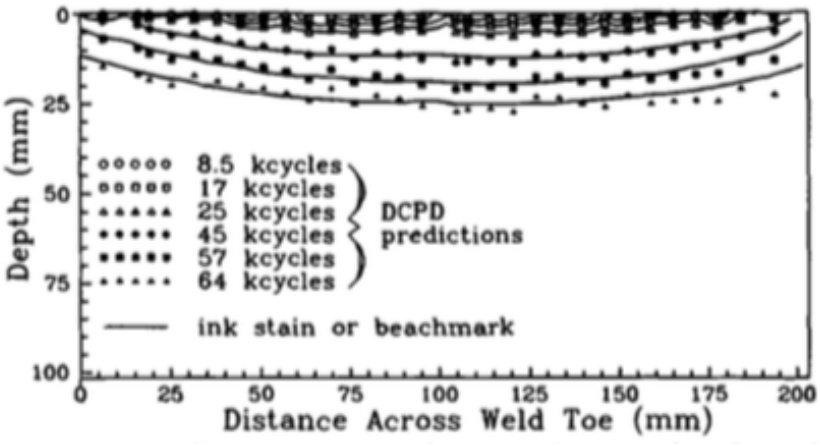

Figure 2.2: Comparison of DCPD measurements to ink stain/beachmark profiles in fatigued steel, taken from Yee and Lambert 1995 (6)

Luukkonen and Ericsson (7) used a five point DCPD probe in order to test for crack formations during a powder metallurgy process. The five point probe as displayed in the paper is shown in Figure 2.3, and has the advantage that the reference probe is very close to the measurement probe. The ratio of the measurement voltage to the reference voltage was measured for several different deviations from the correct press setting, with a larger difference indicating the presence of more severe cracking. Results were obtained for three different specimens: a rectangular bar, an L-shaped bar, and a multilevel component (Figures 2.4 and 2.5).

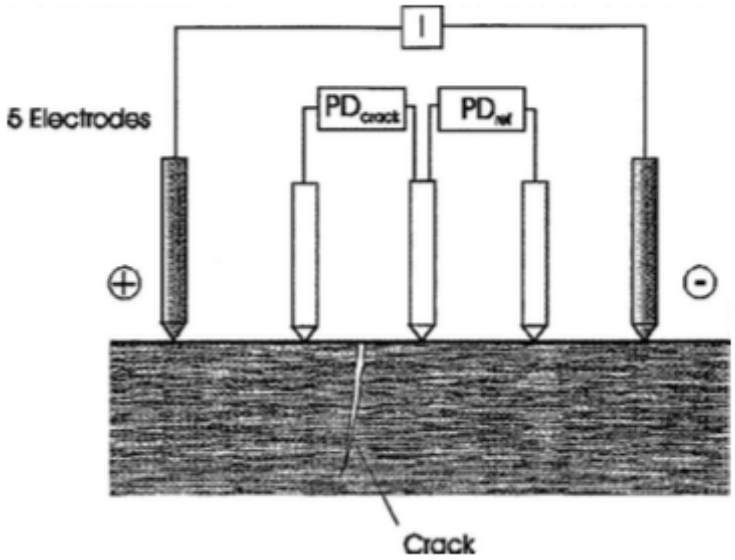

Figure 2.3: The probe configuration used by Luukkonen and Ericsson (7).

2.3 Alternting Current (AC) Potential Drop

2.3.1 Description and Comparisons to other Methods

Alternating current potential drop (ACPD) runs alternating current through the electrodes of the potential drop apparatus and the sample. The alternating current results in the so-called "skin-effect" in the conducting material being tested, meaning the current density decays with the material depth. Because the current goes through a smaller cross-sectional area, a lower current is then required to obtain a larger potential drop than in DCPD. The research described in this section implemented a four-point probe in both theory and measurement.

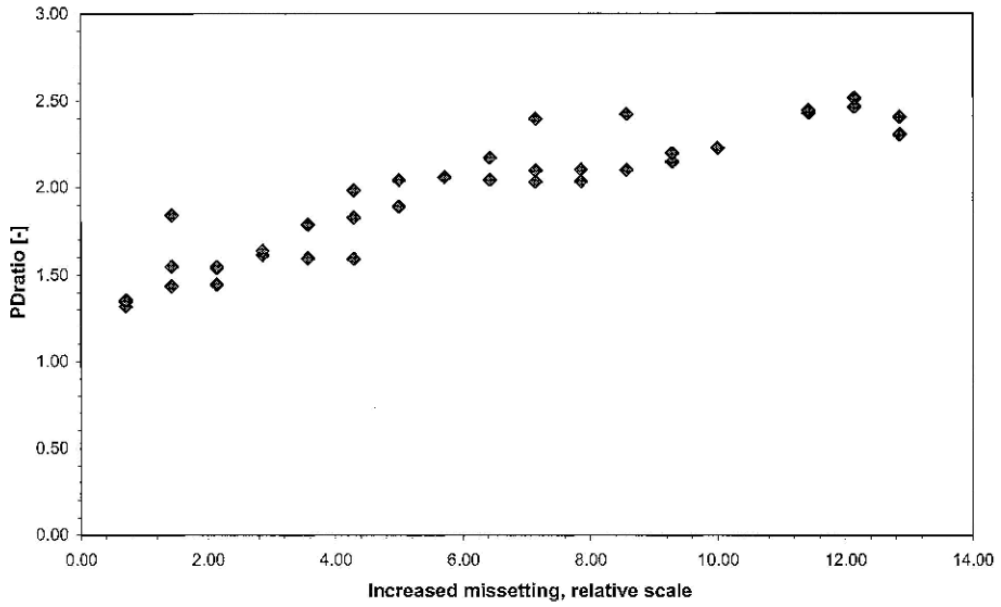

Figure 2.4: The ratio of measured voltage drop to reference voltage for an L-shaped body as a function of missetting, taken from Luukkonen and Ericsson (7).

2.3.2 Measurement Examples

Bowler calculated the electromagnetic field caused by current injected into a conductive half-space (8) and plate (9). The solutions employ the use of transverse magnetic and transverse electric vector potentials, in addition to integral transform methods, to solve Maxwell's equations for the particular set-up. In both papers, the solution is first derived for a single AC current source being injected into the surface of the conductor (see Figure 1.1), and then superposition is utilized to obtain the general solution for a probe situation in which another wire carries the opposite current flowing out.

Bowler and Huang (10) were able to conduct measurements of the electrical conductivity of a number of materials using four-point ACPD measurements. The measurements had the advantage of not requiring a reference probe for calibration, making it useful for field measure-

Table 2.1: Measurements of conductivity by method and metal from (10).

Plate	**Zetec MIZ-120A**	**Eddy Current**	**ACPD**
Brass	16.2 ± 0.3	16.6 ± 0.4	16.42 ± 0.09
Stainless Steel	0.7 ± 0.3	1.31 ± 0.02	1.369 ± 0.007
Spring Steel	-	-	5.50 ± 0.04

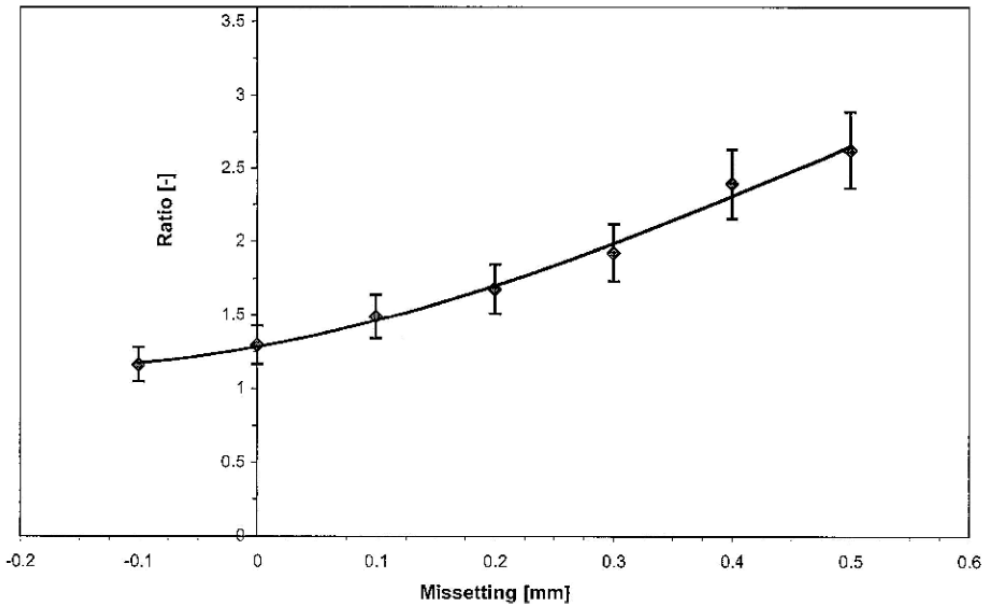

Figure 2.5: The ratio of measured voltage drop to reference voltage for a multi-level body as a function of missetting, taken from Luukkonen and Ericsson (7).

ments. The results also offered better precision than error-corrected broadband eddy current measurements (Table 2.1) and allows for conductivity measurement on ferromagnetic metals whereas eddy current methods do not. The approach was more usable than the prior set-up of a circuit called a Heidweiller bridge which could be used to measure resistivity (equivalently conductivity) in metals, but could not be transported and so was unsuitable for field use.

2.4 Transient Potential Drop

2.4.1 Description

Transient potential drop (TPD) employs the use of an exponential pulsed current injected into the conducting surface. The implications of this were considered in a 2011 paper (11).

2.4.2 Example

One model of TPD (11) examines the effects of an exponential rise current on the voltage drop that occurs on the surface of a conductor. In previous research, frequency dependent solutions for the potential drop had already been obtained for a conductive half space. The

voltage can be expressed, for a colinear configuration with equal spacing between electrodes, as $\Delta V = \frac{I_0}{2\pi\sigma} f(\rho, \omega)$. The frequency dependent function is converted into the time domain by employing the Laplace transform, resulting in

$$\Delta V = \frac{I_0}{2\pi\sigma} f(\rho, t)$$

and

$$\Delta \tilde{V} = \frac{I_0}{2\pi\sigma} \tilde{f}(\rho, \omega).$$

These are then used to find a solution for which the current is an exponential pulse given by $I(t) = I_0[1 - e^{-\frac{t}{\tau}}]$. The result is given by

$$f_\nu(\rho, t) = \frac{\nu}{2\rho}[h(\kappa, \nu, t) - h(\kappa, -\nu, t)],$$

where:

$$h(\kappa, \nu, t) = \frac{1}{\nu} \operatorname{erfc}\left(\frac{\kappa}{2\sqrt{t}}\right) - e^{\nu^2 t}\left[\frac{1}{\nu} e^{\nu\kappa} \operatorname{erfc}\left(\nu\sqrt{t} + \frac{\kappa}{2\sqrt{t}}\right) + \kappa \int_1^\infty \frac{1}{u} e^{\nu\kappa u} \operatorname{erfc}\left(\nu\sqrt{t} + \frac{\kappa u}{2\sqrt{t}}\right) du + \kappa \operatorname{erfc}(\nu\sqrt{t}) \ln \rho\right]$$

and $\nu = -\frac{1}{\tau}$. The method also has the potential to determine conductivity and permeability as functions of depth, and therefore could be used as a tool for characterizing inhomogeneous materials. This is because the Fourier expansion of such a function has an infinite number of terms, allowing a broadband measurement to be carried out.

2.5 Anisotropic Materials

Zhou and Dover (12) analyzed the electromagnetic induction problem as it occurs over an anisotropic half-space. They used an auxiliary vector potential $\vec{A}$, find its Fourier transform $\tilde{A}$, and then solved governing equations for the components of $\tilde{A}$ in order to obtain an algebraic transformed magnetic induction field $\tilde{B}$ in terms of $\tilde{A}$. Then, the case of a solenoid is numerically analyzed, with the relative change in the B-field analyzed as a function of relative change in anisotropy.

Then, a model for uniaxial stress in which the magnetization changed by a factor of $\vec{M} + \zeta\vec{M}$ along one direction was developed.

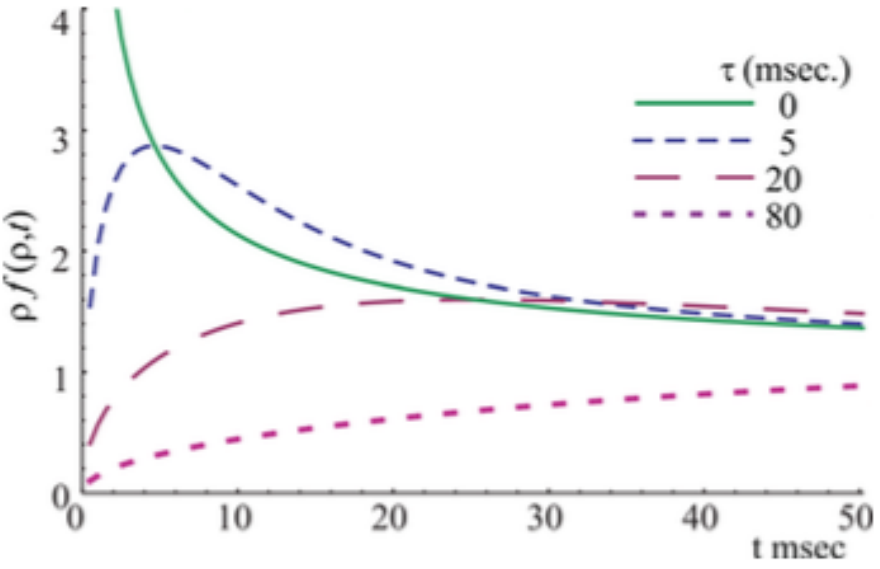

Figure 2.6: Variation in $\rho f(\rho)$, and therefore voltage, as a function of time in the case of a transient current excitation of a four-point probe in contact with a conductor, taken from (11).

Chen, Brennan, and Dover (13) confirmed the validity of certain boundary conditions for an isotropic, infinitely long bar provided that the transverse permeability μ_y replaced μ in the expressions. Then, using a very similar uniaxial stress model as in (12) the relative difference in electric field was derived as a function of anisotropy.

CHAPTER 3. ANALYSIS

3.1 Introduction

In this section, the electrical potential difference between two points on the surface of an anisotropic conducting half space in which two lines of current are injected/extracted perpendicular to the surface by two infinitesimally thin wires is derived. The field is first derived for a single wire, and then another wire is added later by superposition.

3.2 Governing Equation of Electrical Potential due to One Wire

An expression for the electric and magnetic fields in a uniaxially anisotropic space in terms of two auxiliary potentials is given by Felsen and Marcuvitz (14). The expressions given, on modern form, are:

$$\vec{E}(\rho, z) = -i\omega\mu \left[\nabla \times \nabla \times \hat{z} - \left(\frac{\sigma_{tt}}{\sigma_{zz}} - 1 \right) \nabla_z^2 \hat{z} \right] \psi''(\rho, z), z \leq 0 \tag{3.1}$$

where the conductivity is given by the symmetric, second rank tensor (1.7), the transverse gradient operator ∇_z is defined by:

$$\nabla_z = \nabla - \frac{\partial}{\partial z} \hat{z}, \tag{3.2}$$

and $\psi''(\rho, z)$ is the transverse electric potential. The isotropic case from above is the model used by Bowler 2004 (8) and therefore the governing equations for the isotropic case are the same as those stated in that paper in the air region (equation (10) in (8)) is reproduced in (3.3) below.

$$\nabla^2 \nabla_z^2 \psi''(\rho, z) = -\hat{z} \cdot \vec{J}(\rho, z), \ z \leq 0 \text{ (Air)} \tag{3.3}$$

For the governing equations within a sourceless, uniaxially anisotropic medium, we can use Felsen/Marcuvitz, who derived a governing equation for the potential beginning with the governing equations for the electric field discussed in Chapter 1. (14).

$$\left(\frac{\sigma_{zz}}{\sigma_{tt}}\frac{\partial^2}{\partial z^2}+\nabla_z^2+k_{zz}^2\right)\nabla_z^2\psi''(\rho,z)=0,\ z\geq 0\ \text{(Conductor)} \tag{3.4}$$

Setting

$$\Psi(\rho,z)=\nabla_z^2\psi''(\rho,z) \tag{3.5}$$

we obtain from (3.3) and (3.4):

$$\nabla^2\Psi(\rho,z)=-\hat{z}\cdot\vec{J}(\rho,z),\ z\geq 0 \tag{3.6}$$

$$\left(\frac{\sigma_{zz}}{\sigma_{tt}}\frac{\partial^2}{\partial z^2}+\nabla_z^2+k_{zz}^2\right)\Psi(\rho,z)=0,\ z\leq 0 \tag{3.7}$$

Focusing on the conductor region, we can express (3.7) in cylindrical coordinates:

$$\left(\frac{\sigma_{zz}}{\sigma_{tt}}\frac{\partial^2}{\partial z^2}+\frac{\partial^2}{\partial\rho^2}+\frac{1}{\rho}\frac{\partial}{\partial\rho}+k_{zz}^2\right)\Psi(\rho,z)=0 \tag{3.8}$$

The definition of the m-th order Hankel transform with its self inverse is given by:

$$\tilde{f}(\kappa)=\int_0^\infty f(\rho)J_m(\kappa\rho)\rho d\rho \tag{3.9}$$

$$f(\rho)=\int_0^\infty \tilde{f}(\kappa)J_m(\kappa\rho)\kappa d\kappa. \tag{3.10}$$

If $\rho J_0(\kappa\rho)\frac{\partial f(\rho)}{\partial\rho}$ and $\rho f(\rho)\frac{\partial J_0(\kappa\rho)}{\partial\rho}$ vanish at both 0 and ∞, then we have the identity from (15):

$$\int_0^\infty\left[\left(\frac{\partial^2}{\partial\rho^2}+\frac{1}{\rho}\frac{\partial}{\partial\rho}\right)f(\rho)\right]J_0(\kappa\rho)\rho d\rho=-\kappa^2\tilde{f}(\kappa). \tag{3.11}$$

Taking the zeroth-order Hankel transform of (3.8):

$$\begin{aligned}
&\int_0^\infty \left[\left(\frac{\sigma_{zz}}{\sigma_{tt}}\frac{\partial^2}{\partial z^2} + \frac{\partial^2}{\partial \rho^2} + \frac{1}{\rho}\frac{\partial}{\partial \rho} + k_{zz}^2\right)\Psi(\rho, z)\right] J_0(\kappa\rho)\rho d\rho \\
&= \int_0^\infty \left[\left(\frac{\sigma_{zz}}{\sigma_{tt}}\frac{\partial^2}{\partial z^2} + k_{zz}^2\right)\Psi(\rho, z)\right] J_0(\kappa\rho)\rho d\rho + \int_0^\infty \left[\left(\frac{\partial^2}{\partial \rho^2} + \frac{1}{\rho}\frac{\partial}{\partial \rho}\right)\Psi(\rho, z)\right] J_0(\kappa\rho)\rho d\rho \\
&= \left(\frac{\sigma_{zz}}{\sigma_{tt}}\frac{\partial^2}{\partial z^2} + k_{zz}^2\right)\tilde{\Psi}(\kappa, z) - \kappa^2\tilde{\Psi}(\kappa, z) \\
&= \left(\frac{\sigma_{zz}}{\sigma_{tt}}\frac{\partial^2}{\partial z^2} - \gamma^2\right)\tilde{\Psi}(\kappa, z)
\end{aligned} \tag{3.12}$$

where $\gamma^2 = \kappa^2 - k_{zz}^2$ and the identity (3.11) has been used on the second term of the second equation of (3.12), and the RHS of (3.8) now implies a differential equation for $\tilde{\Psi}(\kappa, z)$:

$$\left(\frac{\partial^2}{\partial z^2} - \frac{\sigma_{tt}}{\sigma_{zz}}\gamma^2\right)\tilde{\Psi}(\kappa, z) = 0, z \leq 0. \tag{3.13}$$

3.2.1 Solution to Governing Equation

Let $\sqrt{\frac{\sigma_{tt}}{\sigma_{zz}}}\gamma = \gamma'$. A well-known general solution to (3.13) is:

$$\tilde{\Psi}(\kappa, z) = A(\kappa)e^{-\gamma' z} + B(\kappa)e^{\gamma' z}. \tag{3.14}$$

Since $\Psi(\rho, z)$ must be finite in the limit $z \to \infty$, $B(\kappa)$ must vanish. Thus:

$$\tilde{\Psi}(\kappa, z) = A(\kappa)e^{-\gamma' z} \tag{3.15}$$

Taking the inverse Hankel transform of (3.15) using (3.10), we have:

$$\Psi(\rho, z) = \int_0^\infty A(\kappa)e^{-\gamma' z} J_0(\kappa\rho)\kappa d\kappa \tag{3.16}$$

In order to solve for $A(\kappa)$, we must first deduce some boundary conditions. Suppose the current flowing through the wire is I. If the radius of the wire is a, then the area of the wire/conductor interface is circular and equal to πa^2. Then, assuming no significant skin effect, the current density at the interface ($z = 0$) is given by:

$$J(\rho,0)=\begin{cases}\frac{I}{\pi a^2},\ \rho<a\\ 0,\ \rho>a.\end{cases} \tag{3.17}$$

Since the current runs strictly in the z direction at the conductor surface, we have the constitutive relation:

$$J=\sigma_{zz}E_z \tag{3.18}$$

so that we have the condition, from (3.17) and (3.18), that:

$$E_z(\rho,0)=\begin{cases}\frac{I}{\pi a^2\sigma_{zz}},\ \rho<a\\ 0,\ \rho>a.\end{cases} \tag{3.19}$$

To obtain a boundary condition for $\Psi(\rho,z)$, we must obtain the electric field components in terms of $\Psi(\rho,z)$ and $\psi''(\rho,z)$ using (3.1). Distributing $\psi''(\rho,z)$ through both operators in (3.1) yields:

$$\vec{E}(\rho,z)=-i\omega\mu\left[\nabla\times\nabla\times\hat{z}\psi''(\rho,z)-\left(\frac{\sigma_{tt}}{\sigma_{zz}}-1\right)\nabla_z^2\hat{z}\psi''(\rho,z)\right],z\leq 0. \tag{3.20}$$

The first term in the parentheses in (3.20) is given by:

$$\nabla\times\nabla\times\hat{z}\psi''(\rho,z)=\nabla\times\left[\hat{\rho}\left(\frac{1}{\rho}\frac{\partial\psi''(\rho,z)}{\partial\phi}\right)-\hat{\phi}\left(\frac{\partial\psi''(\rho,z)}{\partial\rho}\right)\right]. \tag{3.21}$$

Using cylindrical symmetry ($\frac{\partial}{\partial\phi}=0$) yields:

$$\nabla\times\nabla\times\hat{z}\psi''(\rho,z)=-\nabla\times\hat{\phi}\left[\frac{\partial\psi''(\rho,z)}{\partial\rho}\right]. \tag{3.22}$$

Taking the curl in (3.22):

$$\nabla\times\nabla\times\hat{z}\psi''(\rho,z)=\hat{\rho}\frac{\partial}{\partial z}\frac{\partial\psi''(\rho,z)}{\partial\rho}-\hat{z}\frac{1}{\rho}\frac{\partial}{\partial\rho}\left[\rho\frac{\partial}{\partial\rho}\psi''(\rho,z)\right]. \tag{3.23}$$

The next goal is to replace the right hand side of (3.23) with more succinct operator notation. By definition, in cylindrical coordinates with cylindrical symmetry ($\frac{\partial}{\partial\phi}=0$), we have:

$$\nabla^2\psi''(\rho,z) = \frac{1}{\rho}\frac{\partial}{\partial\rho}\left(\rho\frac{\partial}{\partial\rho}\psi''(\rho,z)\right) + \frac{\partial^2\psi''(\rho,z)}{\partial z^2}. \tag{3.24}$$

By dropping the z derivative term above, the transverse Laplacian is given by:

$$\nabla_z^2\psi''(\rho,z) = \frac{1}{\rho}\frac{\partial}{\partial\rho}\left[\rho\frac{\partial}{\partial\rho}\psi''(\rho,z)\right]. \tag{3.25}$$

Substituting the LHS of (3.25) for the RHS of (3.23), we obtain:

$$\nabla\times\nabla\times\hat{z}\psi''(\rho,z) = \hat{\rho}\frac{\partial^2\psi''(\rho,z)}{\partial z\partial\rho} - \hat{z}\nabla_z^2\psi''(\rho,z) \tag{3.26}$$

Re-writing (3.20) using (3.26) gives us:

$$\begin{aligned}\vec{E}(\rho,z) &= -i\omega\mu\left[\hat{\rho}\frac{\partial^2\psi''(\rho,z)}{\partial z\partial\rho} - \hat{z}\nabla_z^2\psi''(\rho,z) - \left(\frac{\sigma_{tt}}{\sigma_{zz}}-1\right)\nabla_t^2\hat{z}\psi''(\rho,z)\right]\\ &= -i\omega\mu\left[\hat{\rho}\left(\frac{\partial^2\psi''(\rho,z)}{\partial z\partial\rho}\right) - \hat{z}\frac{\sigma_{tt}}{\sigma_{zz}}\Psi(\rho,z)\right]\end{aligned} \tag{3.27}$$

We can now separate field components in (3.27) to obtain:

$$E_\rho(\rho,z) = -i\omega\mu\frac{\partial^2\psi''(\rho,z)}{\partial z\partial\rho} \tag{3.28}$$

$$E_z(\rho,z) = i\omega\mu\frac{\sigma_{tt}}{\sigma_{zz}}\Psi(\rho,z) \tag{3.29}$$

Using (3.29) in (3.19) gives us a boundary condition for $\Psi(\rho,z)$ at the interface. Recalling that $k_{tt}^2 = i\omega\mu\sigma_{tt}$:

$$\Psi(\rho,0) = \begin{cases}\frac{I}{k_{tt}^2\pi a^2} & \rho < a\\ 0 & \rho > a\end{cases} \tag{3.30}$$

Using (3.16) to replace the potential with the integral gives:

$$\Psi(\rho,0) = \int_0^\infty A(\kappa)J_0(\kappa\rho)\kappa d\kappa = \frac{I}{k_{tt}^2\pi a^2} \tag{3.31}$$

in the $\rho < a$ region. The Fourier-Bessel integral is given by result 6.3.62 in (16):

$$f(\kappa) = \int_0^\infty J_m(\alpha\kappa)\alpha d\alpha \int_0^\infty f(\zeta) J_m(\alpha\zeta)\zeta d\zeta. \tag{3.32}$$

Using (3.32) on (3.31) with $m = 0$ gives:

$$A(\kappa') = \int_0^\infty J_0(\rho\kappa')\rho d\rho \int_0^\infty A(\kappa) J_0(\rho\kappa)\kappa d\kappa = \frac{I}{k_{tt}^2 \pi a^2} \int_0^a J_0(\rho\kappa')\rho d\rho, \tag{3.33}$$

where the limit on the RHS of (3.33) is a since $\Psi(\rho, 0) = 0$ for $\rho > a$. The integral on the RHS can be evaluated (result 9.1.30 in (17)) so that (3.33) becomes:

$$A(\kappa) = \frac{I}{k_{tt}^2 \pi a^2} \left(\frac{a J_1(\kappa a)}{\kappa} \right) = \frac{I}{k_{tt}^2 \pi} \frac{J_1(\kappa a)}{\kappa a}. \tag{3.34}$$

Using the result 9.1.7 in (17):

$$\lim_{z \to 0} J_\nu(z) \sim \left(\frac{z}{2} \right)^\nu \frac{1}{\Gamma(\nu + 1)} \tag{3.35}$$

which, for $\nu = 1$ and $z = a$:

$$\begin{aligned} \lim_{a \to 0} J_\nu(\kappa a) &\sim \frac{\kappa a}{2} \\ \lim_{a \to 0} \frac{J_\nu(\kappa a)}{\kappa a} &\sim \frac{1}{2}. \end{aligned} \tag{3.36}$$

Then for a wire that is allowed to become infinitesimally thin, we have:

$$\lim_{a \to 0} A(\kappa) \sim \frac{I}{2 k_{tt}^2 \pi} \tag{3.37}$$

Inserting the limiting value for $A(\kappa)$(3.37) into (3.16) gives:

$$\Psi(\rho, z) = \frac{I}{2 k_{tt}^2 \pi} \int_0^\infty e^{-\gamma' z} J_0(\kappa\rho)\kappa d\kappa \tag{3.38}$$

We have from (18), result 8.2.23:

$$\int_0^\infty \sqrt{x} e^{-\alpha\sqrt{x^2+\beta^2}} J_0(xy)\sqrt{xy} dx = \frac{\alpha\sqrt{y}}{(y^2+\alpha^2)^{3/2}} e^{-\beta\sqrt{y^2+\alpha^2}} (1 + \beta\sqrt{y^2+\alpha^2}) \tag{3.39}$$

Dividing each side by $\sqrt{y}$, this gives:

$$\int_0^\infty \sqrt{x} e^{-\alpha\sqrt{x^2+\beta^2}} J_0(xy)\sqrt{x} dx = \frac{\alpha}{(y^2+\alpha^2)^{3/2}} e^{-\beta\sqrt{y^2+\alpha^2}} (1 + \beta\sqrt{y^2+\alpha^2}) \tag{3.40}$$

Expression (3.40) applies to (3.38) with $\alpha = \sqrt{\frac{\sigma_{tt}}{\sigma_{zz}}}z$, $x = \kappa$, $y = \rho$, and $\beta = -ik_{zz}$ (we choose a minus sign on β because of the requirement $\Re(\beta^2) > 0$). Let:

$$r' = \sqrt{\rho^2 + \frac{\sigma_{tt}}{\sigma_{zz}}z^2}. \tag{3.41}$$

Using these relations in (3.40) on the integral in (3.38) yields:

$$\Psi(\rho, z) = \frac{I}{2k_{tt}^2\pi}\sqrt{\frac{\sigma_{tt}}{\sigma_{zz}}}\frac{z}{r'^3}e^{ik_{zz}r'}\left(1 - ik_{zz}r'\right) \tag{3.42}$$

3.2.2 Derivation of Electric Field Components for One Wire

Expression (3.42) in conjunction with (3.29) quickly yields a solution for the z component of the electric field:

$$E_z(r') = \frac{I}{2\pi\sigma_{zz}}\sqrt{\frac{\sigma_{tt}}{\sigma_{zz}}}\frac{z}{r'^3}e^{ik_{zz}r'}\left(1 - ik_{zz}r'\right) \tag{3.43}$$

Expression (3.43) reduces to that of the isotropic half space when $\sqrt{\frac{\sigma_{tt}}{\sigma_{zz}}} = 1$ (equation (33) in (8)). To obtain E_ρ, we apply the zero-order Hankel transform to (3.5) and then use the identity (3.11), yielding:

$$\tilde{\psi}''(\kappa, z) = -\frac{\tilde{\Psi}(\kappa, z)}{\kappa^2} \tag{3.44}$$

Which means, using (3.15) with (3.37) on (3.44) , after inverting the transform:

$$\begin{aligned}\psi''(\rho, z) &= \frac{I}{2k_{tt}^2\pi}\int_0^\infty \frac{-1}{\kappa^2}e^{-\gamma' z}J_0(\kappa\rho)\kappa d\kappa \\ &= \frac{I}{2k_{tt}^2\pi}\int_0^\infty \frac{1}{\kappa}e^{-\gamma' z}J_0(\kappa\rho)d\kappa\end{aligned} \tag{3.45}$$

Taking $\frac{\partial}{\partial\rho}$ of (3.45) gives:

$$\frac{\partial\psi''(\rho, z)}{\partial\rho} = \frac{I}{2k_{tt}^2\pi}\int_0^\infty e^{-\gamma' z}J_1(\kappa\rho)d\kappa \tag{3.46}$$

According to result 8.4.9 of (18) we have:

$$\int_0^\infty \frac{1}{\sqrt{x}}e^{-\alpha\sqrt{x^2+\beta^2}}J_1(xy)\sqrt{xy}dx = \frac{1}{\sqrt{y}}\left(e^{-\beta\alpha} - \frac{\alpha}{\sqrt{y^2+\alpha^2}}e^{-\beta\sqrt{y^2+\alpha^2}}\right) \tag{3.47}$$

By canceling the $\sqrt{x}$ terms on the integrand in the left hand side, we obtain:

$$\int_0^\infty e^{-\alpha\sqrt{x^2+\beta^2}} J_1(xy)dx = \frac{1}{y}\left(e^{-\beta\alpha} - \frac{\alpha}{\sqrt{y^2+\alpha^2}} e^{-\beta\sqrt{y^2+\alpha^2}}\right) \tag{3.48}$$

Apply (3.48) to the integral in (3.46) using $\alpha = \sqrt{\frac{\sigma_{tt}}{\sigma_{zz}}}z$, $x = \kappa$, $y = \rho$, and $\beta = -ik_{zz}$ (again, we pick the sign for β based on the requirement $\Re(\beta) > 0$):

$$\frac{\partial\psi''(\rho,z)}{\partial\rho} = \frac{I}{2k_{tt}^2\pi}\frac{1}{\rho}\left(e^{ik_{tt}} - \frac{\sqrt{\frac{\sigma_{tt}}{\sigma_{zz}}}z}{r'} e^{ik_{zz}r'}\right) \tag{3.49}$$

Using (3.28) on (3.49) to obtain $E_\rho(\rho,z)$:

$$E_\rho(\rho,z) = \frac{i\omega\mu I}{2\pi}\frac{1}{ik_{tt}\rho}\left\{e^{ik_{tt}z} - \frac{e^{ik_{zz}r'}}{ik_{zz}r'}\left[1 + \frac{(ik_{tt}z)^2}{ik_{zz}r'}\left(1 - \frac{1}{ik_{zz}r'}\right)\right]\right\} \tag{3.50}$$

It can be checked that, in the isotropic case $\sqrt{\frac{\sigma_{tt}}{\sigma_{zz}}} = 1$, equation (3.50) reduces to the isotropic (40) in (8), given by:

$$E_\rho(\rho,z) = \frac{i\omega\mu I}{2\pi}\frac{1}{ik\rho}\left\{e^{ikz} - \frac{e^{ikr}}{ikr}\left[1 + \frac{(ikz)^2}{ikr}\left(1 - \frac{1}{ikr}\right)\right]\right\}. \tag{3.51}$$

3.2.3 Potential Drop on Surface

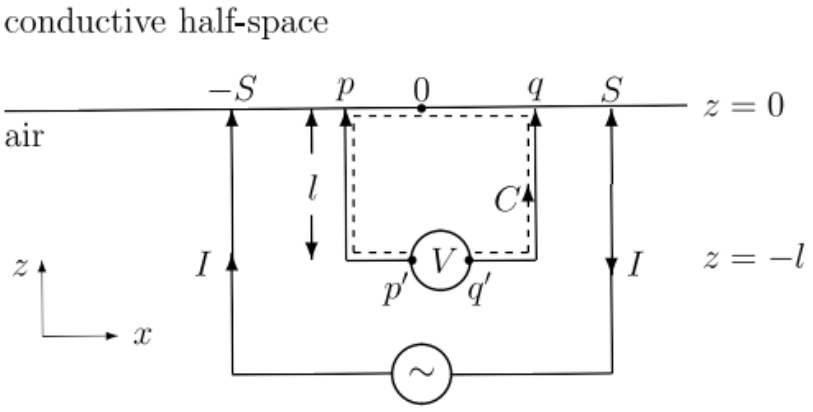

Figure 3.1: Four-point probe configuration with current injected/extracted at $(\pm S, 0, 0)$ and potential drop measured by pins at $x = p$ and $x = q$, taken from (19).

The configuration of a four-point probe in contact with a conductor surface is displayed in Figure (3.1). Wires contact the surface at coordinates $(\pm S, 0, 0)$. Then, the superposed electric field is given by:

$$\vec{E}(\rho, z) = \vec{E}^S(r_+) - \vec{E}^S(r_-) \tag{3.52}$$

where, from (3.41) we have:

$$r_\pm = \sqrt{(x \pm S)^2 + y^2 + z^2} \tag{3.53}$$

Assume that $y = c =$ a constant. Then the voltage from $x = q$ to $x = p$ is given by the line integral:

$$v = -\int_p^q E_x(x, c, 0)dx \tag{3.54}$$

We can find the integrand of (3.54) using:

$$E_x(x, c, 0) = \frac{x + S}{\rho_+} E^S(\rho_+, 0) - \frac{x - S}{\rho_-} E^S(\rho_-, 0) \tag{3.55}$$

where:

$$\rho_\pm = \sqrt{(x \pm S)^2 + c^2} \tag{3.56}$$

Using (3.55) to expand (3.54):

$$v = -\int_p^q \frac{x + S}{\sqrt{(x + S)^2 + c^2}} E_\rho^S(x + S, c, 0)dx + \int_p^q \frac{x - S}{\sqrt{(x - S)^2 + c^2}} E_\rho^S(x - S, c, 0)dx \tag{3.57}$$

Changing the variable to $X = x \pm S$, respectively in (3.57):

$$v = -\int_{p+S}^{q+S} \frac{X}{\sqrt{X^2 + c^2}} E_\rho^S(X, c, 0)dX + \int_{p-S}^{q-S} \frac{X}{\sqrt{X^2 + c^2}} E_\rho^S(X, c, 0)dX \tag{3.58}$$

Then, evaluating $E_\rho(X, c, 0)$ using (3.50) gives:

$$E_\rho^S(X, c, 0) = \frac{I}{2\pi\sqrt{\sigma_{tt}\sigma_{zz}}} \left(\frac{ik_{zz}}{\sqrt{X^2 + c^2}} - \frac{e^{ik_{zz}\sqrt{X^2+c^2}}}{X^2 + c^2} \right) \tag{3.59}$$

Plugging (3.59) into (3.58) gives:

$$\begin{aligned} v = &- \frac{I}{2\pi\sqrt{\sigma_{tt}\sigma_{zz}}}\left(\int_{p+S}^{q+S}\frac{X}{\sqrt{X^2+c^2}}\left[\frac{-ik_{zz}}{\sqrt{X^2+c^2}}+\frac{e^{ik_{zz}\sqrt{X^2+c^2}}}{X^2+c^2}\right]dX\right. \\ &\left.+\int_{p-S}^{q-S}\frac{X}{\sqrt{X^2+c^2}}\left[\frac{-ik_{zz}}{\sqrt{X^2+c^2}}+\frac{e^{ik_{zz}\sqrt{X^2+c^2}}}{X^2+c^2}\right]dX\right) \\ = &-\frac{I}{2\pi\sigma_{tt}}\sqrt{\frac{\sigma_{tt}}{\sigma_{zz}}}\left(\int_{p+S}^{q+S}\left[\frac{-ik_{zz}X}{X^2+c^2}+\frac{Xe^{ik_{zz}\sqrt{X^2+c^2}}}{X^2+c^{2^{3/2}}}\right]dX\right. \\ &\left.+\int_{p-S}^{q-S}\left[\frac{-ik_{zz}X}{X^2+c^2}+\frac{Xe^{ik_{zz}\sqrt{X^2+c^2}}}{X^2+c^{2^{3/2}}}\right]dX\right) \end{aligned} \tag{3.60}$$

We note the identity from result 5.1.1 of (17)

$$\int\frac{e^{ax}}{x^2}dx = \frac{-e^{ax}}{x} - aE_1(-ax) \tag{3.61}$$

Where $E_1(z) = \int_z^\infty \frac{e^{-t}}{t}dt$ is the exponential integral function. Using the change of variable $\alpha = \sqrt{X^2+c^2}$ so that $X = \sqrt{\alpha^2-c^2}$ and $dX = \frac{\alpha d\alpha}{\sqrt{\alpha^2-c^2}}$ on the second term of each integral gives:

$$\begin{aligned} v = &-\frac{I}{2\pi\sqrt{\sigma_{tt}\sigma_{zz}}}\left(\int_{p+S}^{q+S}\frac{-ik_{zz}XdX}{X^2+c^2}+\int_{\sqrt{(p+S)^2+c^2}}^{\sqrt{(q+S)^2+c^2}}\frac{e^{ik_{zz}\alpha}}{\alpha^2}d\alpha\right. \\ &\left.+\int_{p-S}^{q-S}\frac{-ik_{zz}XdX}{X^2+c^2}+\int_{\sqrt{(p-S)^2+c^2}}^{\sqrt{(q-S)^2+c^2}}\frac{e^{ik_{zz}\alpha}}{\alpha^2}d\alpha\right) \end{aligned} \tag{3.62}$$

Finally, using $\int\frac{XdX}{X^2+c^2} = \frac{1}{2}\ln(X^2+c^2)$ and (3.61), we obtain:

$$v = \frac{I}{2\pi\sqrt{\sigma_{tt}\sigma_{zz}}}\left[f(S+q,c) - f(S-q,c) - f(S+p,c) + f(S-p,c)\right] \tag{3.63}$$

where:

$$f(X,c) = f(\rho = \sqrt{X^2+c^2}) = \frac{e^{ik_{zz}\rho}}{\rho} + ik_{zz}[\ln\rho + E_1(-ik_{zz}\rho)]. \tag{3.64}$$

This is in accordance with what had been determined in the isotropic case by (19), where the potential drop was given by:

$$v = \frac{I}{2\pi\sigma}[f_i(S+q,c) - f_i(S-q,c) - f_i(S+p,c) + f_i(S-p,c)], \tag{3.65}$$

where the closed for of f_i is given by:

$$f_{exact}(x,y) = f_{exact}(\rho = \sqrt{x^2+y^2}) = \frac{e^{ik\rho}}{\rho} + ik[\ln\rho + E_1(-ik\rho)]. \tag{3.66}$$

It is seen that the anisotropic case differs in a few respects. The term $\frac{1}{\sqrt{\sigma_{tt}\sigma_{zz}}}$ replaces $\frac{1}{\sigma}$ in the prefactor. The term k_{zz} replaces k throughout.

CHAPTER 4. SUMMARY AND DISCUSSION

4.1 Summary

This paper has derived an expression for the potential drop in a four-point probe placed over an anisotropic space. A few deviations are found in the anisotropic case that distinguish it from the isotropic case. First, the term $\frac{I}{2\pi\sigma}$ becomes $\frac{I}{2\pi\sigma_{tt}}$. Second, another pre-factor term of $\sqrt{\frac{\sigma_{tt}}{\sigma_{zz}}}$ appears in the expression for v. Third, the term $k^2 = -i\omega\mu\sigma$ appearing in the isotropic solution is replaced with $k_{zz}^2 = -i\omega\mu\sigma_{zz}$. These are very simple modifications to the isotropic case and are therefore rather elegant.

In the evaluation of the electric field components, the replacement of σ with σ_{tt} the replacement of k with k_{zz} also holds. In addition, the z term is replaced by $\sqrt{\frac{\sigma_{tt}}{\sigma_{zz}}}z$. Thus, the electric field in the anisotropic case is distorted relative to the electric field in the isotropic case in the z-direction.

4.2 Future Work

This analysis has dealt with the effect of tensor conductivity $\bar{\bar{\sigma}}$ on the electric field distribution and potential drop measured by a four-point probe in the case of a uniaxially anisotropic half-space conductor. A relatively straightforward next step would be to adapt this for a plate conductor exhibiting uniaxial anisotropy. Beyond that, the effects of having a uniaxial anisotropy in permeability, with tensor $\bar{\bar{\mu}}$, may be considered. With tensor $\bar{\bar{\mu}}$, difficulties arise in the manipulation of Maxwell's equations, since $\vec{B}$ cannot be decoupled from $\bar{\bar{\mu}}$ as it can be from μ when trying to obtain a governing equation for the electric field; (1.11) in this analysis.

Further, as was discussed in the literature review, the papers by Zhou and Dover (12) and also by Chen, Brennan, and Dover (13) use models of stress-induced anisotropy which involve

directional changes in the magnetization of the stressed materials. Analysis of how a four-point probe responds to anisotropic permeability via the solutions presented in this paper could be used to conduct stress measurements using the magnetization models of (12) and (13).

BIBLIOGRAPHY

[1] Huang, Yongqiang, "Alternating current potential drop and eddy current methods for non-destructive evaluation of case depth " (2004). Retrospective Theses and Dissertations. Paper 1697.

[2] S. Prajapati, Nagy, P., and Cawley, P., "Potential drop detection of creep damage in the vicinity of welds" NDT& E International, vol. 47, p. 56-65.

[3] Tian, G., Morozov, M., and Takahashi, S. "Pulsed Eddy Current Testing of Thermally Aged and Cold-Rolled Fe-Cu Alloys", IEEE Transactions on Magnetics, vol. 49, no.1, January 2013.

[4] Todorov, E. "Measurement of electromangetic properties of heat exchanger tubes", vol. 48, p. 63-69.

[5] Sposito, G. "Advances in Potential Drop Techniques for Non-Destructive Testing (2009). Non- Destructive Testing Group, Department of Mechanical Engineering, Imperial College, London.

[6] D. Petersen, R. Link, R. Yee and S. Lambert, "A Reversing Direct Current Potential Drop System for Detecting and Sizing Fatigue Cracks along Weld Toes", Journal of Testing and Evaluation, vol. 23, no. 4, p. 254, 1995.

[7] P. Luukkonen and T. Ericsson, "Robust direct current potential drop method to inspect cold pressed green bodies", Powder Metallurgy, vol. 46, no. 4, pp. 329-334, 2003.

[8] N. Bowler, "Analytical solution for the electric field in a half space conductor due to alternating current injected at the surface", Journal of Applied Physics, vol. 95, no. 1, pp. 344-348, 2004.

[9] N. Bowler, "Electric field due to alternating current injected at the surface of a metal plate", Journal of Applied Physics, vol. 96, no. 8, pp. 4607-4613, 2004.

[10] N. Bowler and Y. Huang, "Electrical conductivity measurement of metal plates using broadband eddy-current and four-point methods", Measurement Science and Technology, vol. 16, no. 11, pp. 2193-2200, 2005.

[11] J. Bowler, "Evaluation of the transient potential drop of a four-point probe", Applied Physics Letters, vol. 98, no. 26, art. 264105, 2011.

[12] J. Zhou and W. Dover, "Electromagnetic induction in anisotropic half-space and electromagnetic stress model", Journal of Applied Physics, vol. 83, no. 3, pp. 1694-1701, 1998.

[13] K. Chen, F. Brennan and W. Dover, "Thin-skin AC field in anisotropic rectangular bar and ACPD stress measurement", NDT & E International, vol. 33, no. 5, pp. 317-323, 2000.

[14] L. Felsen and N. Marcuvitz, "Radiation and Scattering of Waves", Prentice-Hall, Inc., 1973.

[15] C. Tranter, Integral transforms in mathematical physics, 1st ed. London: Chapman and Hall, 1974.

[16] P. Morse and H. Feshbach, Methods of Theoretical Physics, 1st ed. New York: McGraw-Hill, 1953.

[17] M. Abramowitz and I. Stegun, Handbook of mathematical functions, with formulas, graphs, and mathematical tables, 1st ed. New York: Dover Publications, 1972.

[18] A. Erdelyi and H. Bateman, Tables of integral transforms, 1st ed. New York: McGraw-Hill, 1954.

[19] N. Bowler, "Theory of four-point alternating current potential drop measurements on a metal half-space", Journal of Physics D: Applied Physics, vol. 39, no. 3, pp. 584-589, 2006.